IEEE *Access*
Multidisciplinary : Rapid Review : Open Access Journal

An Adaptive State of Charge Estimation Method of Lithium-ion Battery Based on Residual Constraint Fading Factor Unscented Kalman Filter

JUQIANG FENG[ID][1,2], FENG CAI[1], JING YANG[1], SHUNLI WANG[ID][3], AND KAIFENG HUANG[2]

[1]State Key Laboratory of Mining Response and Disaster Prevention and Control in Deep Coal Mines, Anhui University of Science and Technology, Huainan 232001, China
[2]School of Mechanical and Electrical Engineering, Huainan Normal University, Huainan 232038, China
[3]School of Information Engineering, Southwest University of Science and Technology, Mianyang 621010, China

Corresponding author: Juqiang Feng (fjq5060912@126.com)

ABSTRACT It is crucial to conduct highly accurate estimation of the state of charge (SOC) of lithium-ion batteries during the real-time monitoring and safety control. Based on residual constraint fading factor unscented Kalman filter, the paper proposes an SOC estimation method to improve the accuracy of online estimating SOC. A priori values of terminal voltage were fitted using cubic Hermite interpolation. In combination with the Thevenin equivalent circuit model, the method of adaptive forgetting factor recursive least squares is used to identify the model parameters. To address the problem of the UKF method strongly influenced by system noise and observation noise, the paper designs an improved method of residual constrained fading factor. Finally, the effectiveness of this method was verified by the test of Hybrid Pulse Power Characteristic and Beijing Bus Dynamic Stress Test. Results show that under HPPC conditions, compared with other methods, the algorithm in the paper estimates that the SOC error of the battery remains between -0.38% and 0.948%, reducing the absolute maximum error by 51.5% at least and the average error by 62.7% at least. Moreover, under the condition of Beijing Bus Dynamic Stress Test the algorithm estimates the SOC error of the battery stays between -0.811% and 0.526%, the SOC estimation errors are all within 0.2% after operation of ten seconds. Compared with other methods, the absolute maximum error can be reduced by 42.7% at least, the average error is reduced by 95% at least. Finally, the test proves that the method is of higher accuracy, better convergence and stronger robustness.

INDEX TERMS Lithium-ion battery, state of charge estimation, residual constraint fading factor- unscented Kalman filter, adaptive forgetting factor recursive least square, cubic Hermite interpolation.

I. INTRODUCTION

At present, new energy vehicles like Tesla, Chinese National Institute of Oceanography (NIO), Xiaopeng and Build Your Dream (BYD), are all powered by lithium-ion batteries because of their long service life, great stability, high energy density, non-pollution and moderate price [1]. However, the capacity of individual lithium-ion battery is not enough to meet the demand for daily driving range of electric vehicles, automobile companies like to use battery packs in series

The associate editor coordinating the review of this manuscript and approving it for publication was Guangya Yang[ID].

or parallel as power sources [2]. Lithium-ion batteries are highly electrochemically non-linear, susceptible to many factors such as operation temperature, charge/discharge current, charge/discharge depth during operation [3]. With no real-time condition monitoring and behavior control, batteries will deteriorate rapidly and even explode, causing unexpected hazards [4]–[6]. As a result, the key technology in doing lithium-ion battery research covers effectively improving the efficiency of lithium-ion batteries, expanding the driving range within a charging cycle, extending the service life of the lithium-ion battery pack, avoiding the battery failures and other problems [7]. In [8], according to the

fractional-order calculus, the authors of this study proposed an SOC and SOH (state of health) co-estimation scheme, established a decomposition equivalent circuit model, used a double fractional-order extended Kalman filter to achieve simultaneous estimation of SOC and SOH. In the presence of initial deviation, noise and disturbance, the maximum steady-state errors of SOC and SOH estimation can be within 1%, ensuring efficient and reliable operation of the battery management system. In [9], based upon incremental capacity analysis (ICA), it proposed a solution for the difficulties in precisely metering SOH of the electric vehicles (EVs). Data set collected from laboratory tests and EVs in people's daily life can be used to have verified the solution, which succeeded in achieving precise estimation of SOH of battery pack in laboratory and EVs in daily life. In [10], and what's more, based on large operating data of real-world EVs, the authors suggested a data-driven charging capacity diagnosis method that charging rate, temperature, State-of-Charge and accumulated driving mileage acted as the inputs, a polynomial feature combination was used for model training, and a CART-based prediction model was built to predict vehicle failures caused by batteries. Directly reflecting the available capacity of the battery, the state of charge (SOC) can be used to calculate and correct the SOH, state of energy (SOE), state of power (SOP), and state of function (SOF) of the battery pack as a whole [11], [12]. Hence, it was of great importance to achieve accurate SOC estimation of Lithium-ion batteries [13]. However, there were no sensors available for measuring the SOC of the battery, it can be only acquired using estimation methods of the model according to the external characteristic parameters of the battery (voltage, current, temperature, etc.) [14], [15].

Normally, SOC estimation methods fall into four categories: ampere-hour integral (AHI) method, parametric characterization method, data-driven method and model-based method. Scholars considered the first two methods as open-loop methods [16], [17]. Besides, Coulomb-counting method was utilized for the connection between the SOC and the cycling of the lithium-ion battery [18]. Nevertheless, despite the easy implementation, error accumulation and the initial SOC value requirement made this method unfit for online SOC estimation [19]. In parametric characterization methods, Open-circuit voltage (OCV) method [20] and electrochemical impedance spectroscopy method [21] was most widely used. In terms of application process, the two methods mentioned above ran essentially the same way, querying the SOC value through a mapping relationship or table [22]. However, these methods were rarely suitable for real time online estimation and used on large scale of BMS because of the long test time, high costs, etc. [23]. In addition, when in use, these methods failed to consider the ageing of the battery, they require regular calibration, otherwise the SOC estimation results will be inaccurate. The data based SOC estimation method mainly includes Artificial Neural Network (ANN) method [24], Support Vector Machine (SVM) method [25], etc. With the SOC estimation accuracy high, it was particularly good at solving non-linear problems, however, it required a large

amount of experimental data as a priori knowledge and all the data should be fully reflective of the battery characteristics. Otherwise, it was most likely to cause over-fitting of the model.

The model-based method of SOC estimation assumed that the battery was a dynamic system, described the state space using battery modelling. Then a variety of filters or observers such as Kalman filter (KF) family algorithms [26], Particle filter (PF) algorithms [27], and nonlinear observer algorithms [28] were used to estimate the state variables. This method was widely used because it enabled the estimation of closed-loop self-calibration and had the advantages of high accuracy and better real-time performance. Especially KF algorithms were intelligent tools to estimate the dynamic state of the battery.

In [29], based on the extended Kalman filter (EKF) and adaptive extended Kalman filter (AEKF), SOC estimation method was established and tested under the federal urban driving schedule of America. In [30], an adaptive improved unscented Kalman filtering (AIUKF) algorithm was developed to realize the iterative calculation process, aiming to overcome the rounding error in the numerical calculation treatment when it was used to estimate the nonlinear state value of the battery pack. In [31], a new SOC estimation method was raised according to a novel safety assurance method based on the compound equivalent modelling and iterative reduction of particle-adaptive Kalman filter. In [32], adopting the forgetting factor recursive least squares (FFRLS) technique, and combining the EKF with the untraced Kalman filter (UKF) for an accurate estimation of battery charge state, SOC estimation accuracy can be reached as high as 2%. In [33], the research proposed a joint online SOC estimation method of the fixed memory recursive least squares (FMRLS) method and Sigma-point Kalman Filter (SPKF) algorithm, and this achieved dynamic identification of model parameters, and battery SOC estimation. Through the above analysis, it was clear that the overall estimation accuracy of KF family algorithms depends on accuracy of equivalent model and the initial parameter, such as initial SOC error, covariance matrix elements.

In the study, we realized an accurate online SOC estimation, and made improvements in the initial value fitting, model parameter identification and SOC estimation methods. The segmented cubic Hermite interpolation method took place of the existing polynomial fitting method in order to obtain continuous smooth open circuit voltages, and to provide quite real a priori values for model identification. Then, the paper introduced forgetting factor optimal mean square error objective function, solving the problems of data saturation and adaptive capability of the RLS method. In contrast with the FFRLS and FMRLS methods in [32] and [33], and the adaptive identification capability of the model became stronger. The UKF transformation process was derived because of EKF, and the introduction of the residual constraint fading factor was done for the UKF method improvement, reducing the influence of system noise
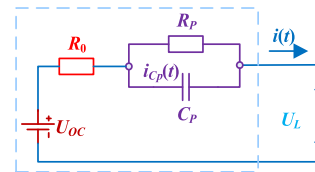
FIGURE 1. Thevenin equivalent circuit model (discharge).

resistance and polarization capacitance of the battery, RC networks describe the slowly changing concentration polarization within a battery. U_L represents the terminal voltage.

From Fig.1, defining the power battery charging current as positive and the discharging current as negative, the mathematical expression of the model is expressed as follows

$$\begin{cases} \dot{U}_p(t) = -\dfrac{U_p(t)}{R_p C_p} + \dfrac{1}{R_p} i(t) \\ U_L(t) = U_{oc} + i(t) R_0 + U_p(t) \end{cases} \quad (2)$$

In Eq (2), U_p(t) is the voltage across the RC network, which reflects a polarized electromotive force of the battery. U_L(t) and i(t) are measured with the sensors and are discrete data. U_{oc}, R_0, R_p and C_p are unknown parameters to be identified online by the adaptive forgetting factor recursive least squares. After discretization of Eq.2, a difference equation (3) is achieved as follows

$$U_L(s) = U_{oc}(s) + i(s)(R_0 + \dfrac{R_p}{1 + R_p C_p s}) \quad (3)$$

U_L(s) − U_{oc}(s) in the following equation is defined as the system output, i(s) is defined as the system input, and the transfer function of the system is rewritten as the equation (4)

$$G(s) = \dfrac{U_L(s) - U_{oc}(s)}{i(s)} = R_0 + \dfrac{R_p}{1 + R_p C_p s} \quad (4)$$

After a bilinear transformation, the transfer function of the system is converted to the Z-domain, and the equation (5) is decided.

$$G(z^{-1}) = \dfrac{a_2 + a_3 z^{-1}}{1 + a_1 z^{-1}} \quad (5)$$

Eq. (5) satisfies Eq. (6).

$$\begin{cases} a_1 = \dfrac{T - 2R_p C_p}{T + 2R_p C_p}, a_2 = \dfrac{R_0 T + R_p T + 2R_0 R_p C_p}{T + 2R_p C_p} \\ a_3 = \dfrac{R_0 T + R_p T - 2R_0 R_p C_p}{T + 2R_p C_p} \end{cases} \quad (6)$$

where T is the sampling time. It is assumed that U_{oc} and R_0 stay constant during a sampling period because the sampling time is very short. Then a discretization formula (7) of the model is obtained through the inversion of Z.

$$U_L(k) = U_{oc}(k) - a_1[U_L(k-1) - U_{oc}(k-1)] \\ + a_2 i(k) + a_3 i(k-1) \quad (7)$$

where a_1, a_2 and a_3 are coefficients of the equation to be identified.

II. BATTERY MODELLING AND PARAMETERS IDENTIFICATION

A. BATTERY MODELLING

For Model-based methods of SOC estimation, it needs a model first, and the model may describe the external characteristics of the power battery accurately. The widely used models include electrochemical model, empirical model and equivalent circuit model.

The electrochemical model is a battery model based on porous electrodes and solution concentration theory [34], and the terminal voltage and SOC of the battery can be calculated according to the electrochemical reaction process. The Pseudo-2-Dimensinal (P2D) model, most typical, uses a set of coupled partial differential equations to describe the concentration and potential of solid-phase lithium-ion batteries [35]. Though this model with high accuracy mainly reflects the internal chemical reaction mechanism of the battery, it is hard to realize an accurate estimation just for numerous parameters, and its computational complexity is high and time-consuming [36]. In [37], it presented certain simplified electrochemical models such as the Nerst model, Shepherd model and Unnewehr model. The simplified electrochemical models are from the practice, and they are referred to by scholars as empirical models. In [29] and [38], a new combined model was proposed combining the Nerst, Shepherd and Unnewehr models. The equation of the model is shown as follows

$$U_{oc} = k_0 - R_0^* I - k_1^* x + k_2/x + k_3^* \ln(x) - k_4 \ln(1-x) \quad (1)$$

where U_{oc} means the OCV of the battery, $k_{1,2,3,4}$ are the coefficients of polynomial equation respectively, and x the SOC of the battery.

The equivalent circuit model consists of conventional circuit elements such as resistors, capacitors and constant voltage sources, uses an RC network to describe the dynamics of the power battery. With higher applicability to various operating conditions, it is easy for analysis and application. Considering an appropriate trade-off between accuracy and complexity, the study selects Thevenin equivalent circuit model for lithium-ion battery as the battery model in the study. Physically simple and clear, this model can be used to simulate charging and discharging characteristics of the battery. The specific circuit is shown in Fig. 1.

In Fig.1 i(t) is the load current. R_0 is the internal ohmic resistance to describe the rapidly changing ohmic polarization within the battery. R_p and C_p are respectively polarization

B. SEGMENTED CUBIC HERMITE INTERPOLATION

We need to obtain $U_{oc}(k)$ as an a priori value in order to identify the model parameters. It is usual that a polynomial fit method to the SOC-OCV discrete data is used to obtain the value of $U_{oc}(k)$. But this method failed to ensure that all the OCV test points fall on the fitted curve and the modelling accuracy is low accordingly [39], [40]. The study we did uses a segmented cubic Hermite interpolation to fit the SOC-OCV curve for reliability of the a priori value.

The segmented cubic Hermite interpolation method enables the interpolation points to be within the interpolation function, ensuring that there are the same first, second and even higher order derivatives are available at each interpolation points. Therefore, this method made the interpolation points continuous smooth, also reflected the real changes of the data well. For the changes of each parameter in the equivalent model of the lithium battery, these changes are non-linear, and especially irregular. It is more scientific and accurate that segmented cubic Hermite interpolation is adopted to approximate the real variation of the parameters.

It is assumed there exist nodes x_i within any interval $[a, b]$ and $i = 0, 1, \cdots n$, $a = x_0 < x_1 < \cdots < x_n < b$, and a derivative value y_i'.

For any two vectors of nodes to be interpolated (x_i, y_i) and (x_{i+1}, y_{i+1}), here x_i means the measurement of the SOC, y_i the value of the corresponding function OCV. The distance of i decided as h_i and the primary difference quotient as δ_i, as is shown in Eq. (8)

$$h_i = x_{i+1} - x_i, \delta_i = \frac{y_{i+1} - y_i}{h_i} \tag{8}$$

Now it is decided that variable s equals x-x_i, and that h equals h_i, a function expression of segmented cubic Hermite interpolation is shown in Eq. (9)

$$H(x) = \frac{3h^2 - 2s^2}{h^3} y_{i+1} + \frac{h^3 - 3hs^2 + 2s^3}{h^3} y_i$$
$$+ \frac{s^2(s - h)}{h^2} d_{i+1} + \frac{s(s - h)^2}{h^2} d_i \tag{9}$$

and Eq. (9) satisfies Eq. (10).

$$H(x_i) = y_i, H(x_{i+1}) = y_{i+1}, H'(x_i) = d_i, H'(x_{i+1}) = d_{i+1} \tag{10}$$

where d_i and d_{i+1} are the derivation value of y_i, y_{i+1} respectively, which can be approximated by the difference quotient operations of the nodes before and after the interpolation points.

C. FORGETTING FACTOR RECURSIVE LEAST SQUARES METHOD

Easy to understand and fast to converge, least square (LS) method is widely used in the parameter identification for the equivalent circuit model of lithium-ion batteries. An expression of the difference equation is shown in Eq. (11)

$$y_k = h(k)^T \theta(k) + v(k) \tag{11}$$

where $h(k)^T$ is an observable quantity, $\theta(k)$ is a vector of parameters with discrimination, $v(k)$ is system noise.

From Eq. (7) and Eq. (11) comes the least square expression of the Thevenin model as shown in Eq. (12)

$$\begin{cases} y_k = U_L(k) \\ h(k) = [\, 1 \ U_{oc}(k - 1) - U_L(k - 1) \ i(k) \ i(k - 1) \,]^T \\ \theta(k) = [\, U_{oc}(k) \ a_1 \ a_2 \ a_3 \,]^T \end{cases} \tag{12}$$

where U_{oc} $(k$-1) denotes the open circuit voltage input at the time k-1, U_L $(k$-1) the terminal voltage input at the time k-1, and $i(k)$ denotes the current input at the time k.

In the process of online identification, the latest data should be input and output constantly, and the estimation accuracy of θ is improved by continuous iteration until a satisfactory accuracy is achieved. For the system model and parameters greatly influenced by external factors, the method can accurately capture the real-time characteristics of the system by automatically correcting and updating the system parameters. However, with the times of algorithm data iterations increasing, data saturation may occur. As a result, a method of forgetting factor recursive least squares in [41] was purposed for an improvement of the online estimation capability of the RLS algorithm. According to Eq. (11), extending y_k and $h(k)$ to N dimensions, and introducing the noise error $e(k)$, the residual sum of squares is required to be minimal according to the principle of recursive least squares, and a formula for FFRLS for recursive operations are obtained finally. See Eq. (13)

$$\begin{cases} \theta(k) = \theta(k - 1) + K(k) \left[y(k) - h(k)^T \theta(k - 1) \right] \\ K(k) = \dfrac{P(k - 1) h(k)}{\lambda + h^T(k) P(k - 1) h(k)} \\ P(k) = \lambda^{-1} \left[I - K(k) h^T(k) \right] P(k - 1) \end{cases} \tag{13}$$

where $\hat{\theta}(k)$ is the estimated value of the model parameters at the time k, $K(k)$ the gain matrix at the time k, $P(k)$ the updated covariance matrix at the time k, and λ the forgetting factor ranging from 0-1, the closer the factor is to 1, the better the simulation.

D. ADAPTIVE FORGETTING FACTOR PROCESSING

Batteries are non-linear, changes in current input and external noise do not maintain a certain predictable trend, and errors in the calculation will vary with time. Therefore, according to the system characteristics, battery operation at different stages requires different forgetting factors. A simple RLS approach with a fixed forgetting factor failed to meet the needs of different operation conditions and stages of the electric vehicle. Reference [42] proposed a variable forgetting factor (VFF) strategy using an exponential curve approach to describe the forgetting factor changing with error, and the FFRLS performance was improved. While in [43], there raised a Limited Memory RLS algorithm for the purpose of modulating the error covariance matrix in real time by adding a fading factor to weaken the effect of old data. Through the
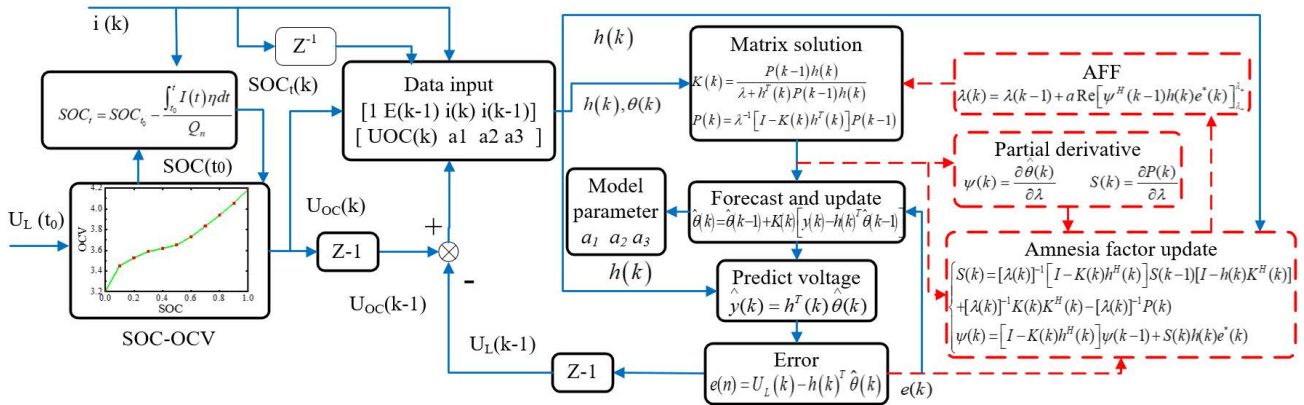
FIGURE 2. Computational flowchart of the AFFRLS online identification method.

above research, we introduces the RLS method with adaptive forgetting factor (AFF) to obtain the optimal forgetting factor by solving for the minimum estimation of the prior error. Then, data saturation can be overcome and there will be adaptive online identification of parameters [44].

The AFFRLS method aims to calculate λ that optimizes the mean squares of priori error. Therefore, the cost function is determined as shown in Eq. (14).

$$J'(n) = \frac{1}{2}E[|e(k)|^2], \; e(k) = U_L(k) - h(k)^T \theta(k) \quad (14)$$

where $e(k)$ is a priori error referred to above, $E[\;]$ is the expectation operator.

The partial derivative of $J'(n)$ in Eq. (14) with respect to λ is completed for optimization, see Eq. (15).

$$\begin{aligned}\nabla_\lambda(k) &= \frac{\partial J'(k)}{\partial \lambda} = \frac{1}{2}E\left[\frac{\partial e(k)}{\partial \lambda}e^*(k) + \frac{\partial e^*(k)}{\partial \lambda}e(k)\right]\\&= -\frac{1}{2}E\left[\psi^H(k-1)h(k)e^*(k) + h^H(k)\psi(k-1)e(k)\right]\end{aligned}$$
$$(15)$$

where $\Psi(k)$ is the derivative of the estimated vector with respect to λ, and $S(k)$ the derivative of the covariance matrix with respect to λ. The superscript symbol H indicates a transpose, and he superscript symbol $*$ the accompanying matrix. According to the ''method of steepest descent,'' we can use the recursive form of Eq. (16) to express the forgetting factor as in the following equation.

$$\begin{aligned}\lambda(k) &= \lambda(k-1) - a\hat{\nabla}_\lambda(k) = \lambda(k-1)\\&\quad + aRe\left[\psi^H(k-1)h(k)e^*(k)\right]_{\lambda_-}^{\lambda_+}\end{aligned} \quad (16)$$

where a is a small, positive learning-rate parameter. λ_+ denotes the upper limit, while λ_- the lower limit.

In summary, the update process of the adaptive forgetting factor of AFFRLS is expressed as follows

$$\begin{cases}S(k) = [\lambda(k)]^{-1}\left[I - K(k)h^H(k)\right]S(k-1)[I - h(k)K^H(k)]\\+[\lambda(k)]^{-1}K(k)K^H(k) - [\lambda(k)]^{-1}P(k)\\\psi(k) = \left[I - K(k)h^H(k)\right]\psi(k-1) + S(k)h(k)e^*(k)\end{cases}$$
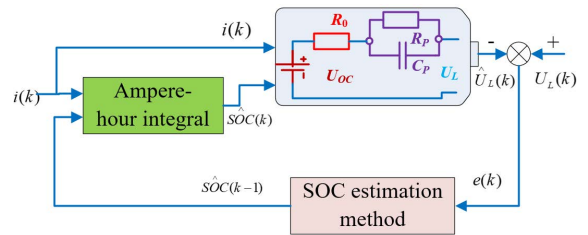$$(17)$$

FIGURE 3. Thevenin equivalent circuit model (discharge).

From the above analysis, it can be intuitively found that the variable forgetting factor becomes smaller when the priori error $e(n)$ deviation grows larger. On the contrary, the corresponding variable forgetting factor becomes larger when the estimation deviation becomes smaller. Then, the gain matrix and variance matrix can be corrected through changes of forgetting factor. Therefore, the specific flow chart for identifying the parameters in Thevenin model using the AFFRLS method is shown in Fig. 2.

As shown in Fig.2, the calculation process in the black scheme is the online identification method FFRLS, and the calculation process in the red scheme with dotted line is a improved method proposed in the paper. From the calculation process in Fig.2 and Eq. (8), we can invert the values of R_0, R_p and C_p, as shown in Eq. (18).

$$R_0 = \frac{a_3 - a_2}{a_1 - 1}, \; R_p = \frac{2(a_1 a_2 - a_3)}{a_1^2 - 1}, \; C_p = \frac{T(a_1^2 - 2a_1 + 1)}{4(a_3 - a_1 a_2)}$$
$$(18)$$

where a_1, a_2 and a_3 were defined in the Eq. (7).

III. ESTIMATION OF BATTERY STATE OF CHARGE

The interior of the lithium-ion battery is a typical nonlinear system. A closed-loop system is constructed in the study in order to obtain the internal state parameters, as is shown in Fig.3.

where i(k) and U_L(k) mean the input current, the voltage at the output at the time k respectively. $\hat{U}_L(k)$ and e(k) are the estimated value of the terminal voltage at the time k and the

error respectively, $S\hat{O}C(k)$ is the estimate of the SOC at the time k.

A. ESTIMATE BATTERY SOC BASED ON EKF

EKF method aims at transformation of the state equation of the nonlinear system into a linear one. In the process of expanding the nonlinear discrete function, the second-order and higher-order functions are discarded, and an approximate linear space equation is obtained after linearization of the equation [16]–[45]. The general expression for the linearized equation is shown as follows

$$\begin{cases} x_k = A_{k-1}x_{k-1} + B_{k-1}u_{k-1} + w_{k-1} \\ y_k = C_k x_k + D_k u_{k-1} + v_k \end{cases} \quad (19)$$

where x_k is the state vector, y_k is the observation vector, u_k is the input vector, w_k and v_k are independent Gaussian white noises. The first part of the equation represents the state equation, and the second part means the observation equation. A_k is the state transfer matrix, B_k the input matrix, C_k the observation matrix, and D_k the direct transfer matrix.

Combined with the Thevenin equivalent circuit model, the voltages U_p and the SOC in the model work as state variables of the system, the terminal voltage U_L of the battery as the system observation, and the charge/discharge current i as the system excitation. With the Euler's formula, a discrete state equation of the system is obtained from Eq. (20) and AHI method [47], as is shown in Eq. (20).

$$\begin{cases} \begin{bmatrix} SOC_k \\ U_{p,k} \end{bmatrix} = \begin{bmatrix} 1 & 0 \\ 0 & e^{-T/\tau} \end{bmatrix} \begin{bmatrix} SOC_{k-1} \\ U_{p,k} \end{bmatrix} \\ + \begin{bmatrix} T/Q_n \\ R_p(1-e^{-T/\tau}) \end{bmatrix} i_{k-1} \\ U_{L,k} = U_{oc}(SOC_k) + i_k R_{0,k} + U_{p,k} \end{cases} \quad (20)$$

where k is the time point, SOC_k the state value at the k time point, T the period specified during the experiment, and τ the time constant, reflecting the speed of response changes in the circuit, $\tau = R_p C_p$. $U_{OC}(SOC_k)$ denotes the nonlinear function relationship between SOC and OCV, $U_{L,k}$ is the terminal voltage at the time k, Q_n is the rated capacity of the battery. Combining Eq. (19) and Eq. (20), the coefficient matrix is expressed as follows

$$\begin{cases} A_{k-1} = \begin{bmatrix} 1 & 0 \\ 0 & e^{-T/\tau} \end{bmatrix}, B_{k-1} = \begin{bmatrix} T/Q_0 \\ R_p(1-e^{-T/\tau}) \end{bmatrix} \\ C_k = \begin{bmatrix} \dfrac{\partial U_{oc}(SOC_k)}{\partial SOC} & -1 \end{bmatrix}, D_k = \begin{bmatrix} R_{0,k} \end{bmatrix} \end{cases} \quad (21)$$

For the linearized model and matrix of the coefficients, the basic formula of the KF algorithm is used to get the recursive process of an extended Kalman filter, as is shown in Eq. (22).

$$\begin{cases} \hat{x}_k^- = f(x_k) \\ \hat{P}_k^- = A_{k-1}\hat{P}_{k-1}A_{k-1}^T + Q_k \\ K_k = \hat{P}_k^- C_k^T (C_k \hat{P}_k^- C_k^T + R_k)^{-1} \\ \hat{x}_k = x_k^- + K_k[y_k - h(x_k^-)] \\ \hat{P}_k = [I + K_k C_k]\hat{P}_k^- \end{cases} \quad (22)$$

where P represents the mean square error, K the Kalman gain, I the identity matrix, and R and Q the expected value of observation noise v and process noise w respectively.

B. ESTIMATE BATTERY SOC BASED ON UKF

The battery's open circuit voltage, internal resistance, terminal voltage, and state of charge show the strong nonlinear changes under battery operating conditions. For strong nonlinear systems, EKF will fail, requiring stronger estimation methods: the sigma-point approach in those cases was often preferred, as stated in [11], [48], and [49]. Although, the sigma-point approach was conceptually more complex than the EKF, but its computational complexity was identical to the EKF. This was mainly because the Jacobian matrix was solved unnecessarily when approximating a non-linear function. And it did not ignore higher order terms either, and enjoyed a higher computational accuracy for the each nonlinear statistics.

Steps of estimate battery SOC are based on UKF [50]:
(1) Initialization of UKF:

$$\begin{cases} \hat{x}_{(0)} = E(x_0) \\ P_{x(0)} = E[(x_0 - \bar{x})(x_0 - \bar{x})^T] \end{cases} \quad (23)$$

where $\hat{x}_{(0)}$ is the variance of x_0, $P_{x(0)}$ is the covariance of x_0. The state vector x_k contains SOC and U_p. The initial value of SOC is obtained from the SOC-OCV curve by looking up the table. When U_p initial value is zero, the polarization effect of the battery at the initial moment is minimized.

(2) Updating status time:
Sigma-point is acquired in Eq. (24)

$$\begin{cases} \chi^{(0)} = \bar{x} \\ \chi^{(i)} = \bar{x} + \sqrt{(n+l)P_x}, i = 1, 2, \ldots, n \\ \chi^{(i)} = \bar{x} - \sqrt{(n+l)P_x}, i = n+1, n+2, \ldots, 2n \end{cases} \quad (24)$$

where $\bar{x}$ is the mean value of variable x at the n-dimensional state, P_x the covariance, and λ the scaling factor. Then weighting factors is calculated as follows

$$\begin{cases} w_m^{(0)} = \dfrac{l}{n+l}, l = a^2(n+k) - n \\ w_c^{(0)} = \dfrac{l}{n+l} + (1 - a^2 + b) \\ w_m^{(i)} = w_c^{(i)}\dfrac{l}{2(n+l)}, i = 1, L, 2n \end{cases} \quad (25)$$

where ω_m and ω_c are the weights needed to calculate the mean and variance of the Sigma points respectively. The scale factor α is used to determine the distribution of Sigma points.

And β is a non-negative weight, reducing a parameter of higher order errors.

And status time is updated. See Eq. (26)

$$\hat{x}_{(k|k-1)} = \sum_{i=0}^{2n} w_{(i)}^m \chi_{(k|k-1)}^i \qquad (26)$$

(3) Errors is updated as shown in (27):

$$P_{(k|k-1)} = \sum_{i=0}^{2n} w_{(i)}^c (\chi_{(k|k-1)}^i - \hat{x}_{(k|k-1)})$$
$$(\chi_{(k|k-1)}^i - \hat{x}_{(k|k-1)})^T + Q_k \qquad (27)$$

(4) The priori is estimated as listed in (28):

$$\hat{y}_{(k|k-1)} = \sum_{i=0}^{2n} w_{(i)}^m y_{(k|k-1)}^i \qquad (28)$$

(5) Gain updated is found in (29):

$$K_{(k)} = \sum_{i=0}^{2n} w_{(i)}^c (\chi_{(k|k-1)}^i - \hat{x}_{(k|k-1)})(\chi_{(k|k-1)}^i - \hat{x}_{(k|k-1)})^T$$
$$[\sum_{i=0}^{2n} w_{(i)}^c (\chi_{(k|k-1)}^i - \hat{x}_{(k|k-1)})(\chi_{(k|k-1)}^i - \hat{x}_{(k|k-1)})^T + R_{(k)}]^{-1}$$
$$(29)$$

(6) The state estimation is updated, See Eq. (29)

$$\hat{x}_{(k)} = \hat{x}_{(k|k-1)} + K_{(k)}(y_{(k)} - \hat{y}_{(k|k-1)}) \qquad (30)$$

(7) The posterior covariance is calculated in Eq. (31)

$$P_{(k)} = P_{(k|k-1)} - K_{(k)} P_{(k)} K_{(k)}^T \qquad (31)$$

C. ONLIN ESTIMATE BATTERY SOC BASED ON RCFF-UKF
1) ESTIMATE BATTERY SOC BASED ON RCFF-UKF
UKF method achieves nonlinear filtering through "approximate probability," without linearization operation of nonlinear system, and it has ideal filtering accuracy. However, this method is very sensitive to the noise model of the system. Lithium-ion batteries are affected by temperature, charge and discharge ratio, charge and discharge times and other factors, so the state noise and observation noise of the system are colored noise rather than zero-mean Gaussian white noise as we usually think. Therefore, the paper introduced the idea of fading memory with residual constraint [51], [52] to enhance the correction of strategy information through the weighted processing of the estimation error covariance matrix of UKF, and the divergence of filtering can be suppressed, the stability of UKF can be improved accordingly.

The transformation of the error update in the UKF method of Eq. (27) forms the following results (Eq.32):

$$\begin{cases} P_{(k|k-1)} = LMD_k \sum_{i=0}^{2n} w_{(i)}^c (\chi_{(k|k-1)}^i - \hat{x}_{(k|k-1)}) \\ (\chi_{(k|k-1)}^i - \hat{x}_{(k|k-1)})^T + Q_k \\ LMD_k = diag[\eta_{1,k}, \eta_{2,k} \cdots, \eta_{n,k}] \end{cases} \qquad (32)$$

where LMD_k is the diagonal asymptotic array, and η_i the asymptotic factor.

Residual constraint fading memory UKF is very strong about robustness to the variation of real system parameters. The sufficient condition for making the non-polar Karl filter a residual constraint is to determine the time-varying gain array K_k online, where the conditions are as follows:

$$\begin{cases} E[x_k - \hat{x}_k][x_k - \hat{x}_k]^T = \min \\ E[\varepsilon_k \varepsilon_{k+j}^T] = 0 \; k = 1, 2, \cdots, j = 1, 2, \cdots \end{cases} \qquad (33)$$

where ε_k is the sequence of observation residuals, derived from the vector of state estimates at the time k, which contains the information obtained from the observation vector y_k at the time k. An equation is expressed as follows:

$$\varepsilon_k = y_k - h(\hat{x}_k, v_k) \qquad (34)$$

where v_k is the observation noise.

From the priori knowledge of the system, the ratio of the individual state fading factors in η_i is determined to be the following equation:

$$\eta_{1,k} : \eta_{2,k} : \cdots \eta_{n,k} = a_1 : a_2 \cdots a_n \qquad (35)$$

where a_i is the scale factor. Let η_i equal to $a_{i*} c_k$, and if the common factor c_k to be determined can be solved, an asymptotic array LMD_k is obtained.

By the filter optimality principle and after a series of derivations, c_k is obtained as follows:

$$c_k = \frac{tr[c_{0,k} - R_k]}{\sum_j^n a_j [\sum_{i=0}^{2n} w_{(i)}^c (y_{i,k} - \hat{y}_{i,k})(y_{i,k} - \hat{y}_{i,k})^T]_{jj}} \qquad (36)$$

This leads to the derivation of $\eta_{i,k}$ in the asymptotic array as in Eq.(37):

$$\eta_{i,k} = \begin{cases} a_i c_k & a_i c_k \geq 1 \\ 1 & a_i c_k < 1 \end{cases} \qquad (37)$$

The update formula for the residual array $c_{0,k}$ is listed in the following equation:

$$c_{0,k} = \begin{cases} \varepsilon_1 \varepsilon_1^T & k = 0 \\ \rho c_{0,k} + \varepsilon_{k+1} \varepsilon_{k+1}^T / (1 + \rho) & k \geq 1 \end{cases} \qquad (38)$$

where ρ is the forgetting factor and takes values from 0 to 1. The larger the value is, the smaller the proportion of information available before the time k, and the more prominent the influence of the current residual vector. Therefore, it is quite able to track sudden changes in state.

Combining the relevant equations and ideas, the paper composed the SOC estimation method based on RCFF-UKF for lithium-ion batteries, and a calculation flow chart obtained is shown in Fig. 4.

In Fig. 4, the calculation in the black solid line box is Kalman Filter method, the calculation in the light blue dotted line box is UKF method, and the calculation in the red dotted line box is an improved method proposed by the paper.
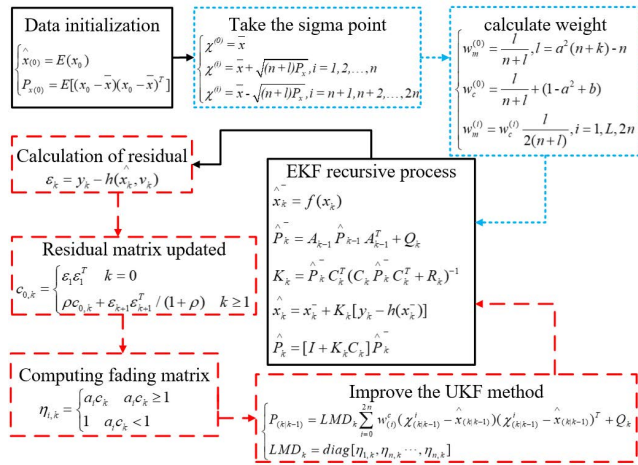
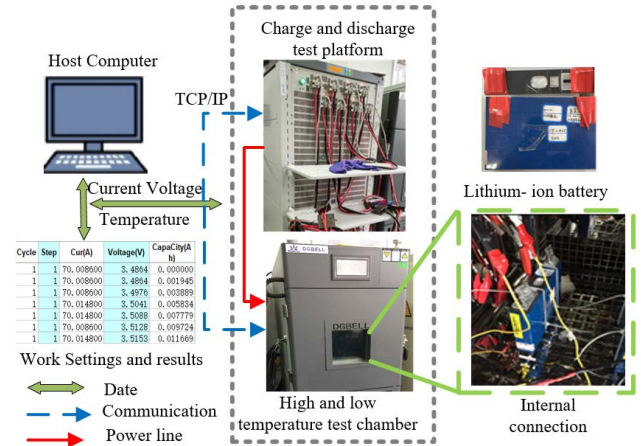**FIGURE 4.** Flow chart of estimate battery SOC based on RCFF-UKF.

FIGURE 5. Core idea of the flow chart of algorithm.

FIGURE 6. Schematic diagram of battery charge and discharge test platform.

FIGURE 7. Current and voltage values of HPPC.

2) ONLINE ESTIMATE BATTERY SOC

When used, Lithium-ion battery is of time-variant characteristic. The model parameters of the battery change constantly under different SOC, charge-discharge ratio, temperature and aging conditions. So what is actually necessary is a joint algorithm of online self-adaptive parameter identification of the battery and SOC estimation model. And the paper proposes a flow chart of the joint algorithm as shown in Fig. 5:

Fig. 5 shows that a method described in the red dotted line. The highlights of the paper contain the following three parts. (1) The method of cubic Hermite interpolation is adopted to improve the fitting accuracy of SOC-OCV. (2) AFF-RLS identification method is used to improve the parameter identification accuracy of lithium-ion battery model, and to provide an accurate model for online SOC estimation of the battery. (3) The UKF method improved can improve the SOC estimation accuracy, and reduce the sensitivity of noise and initial value, and achieve strong robustness of the system.
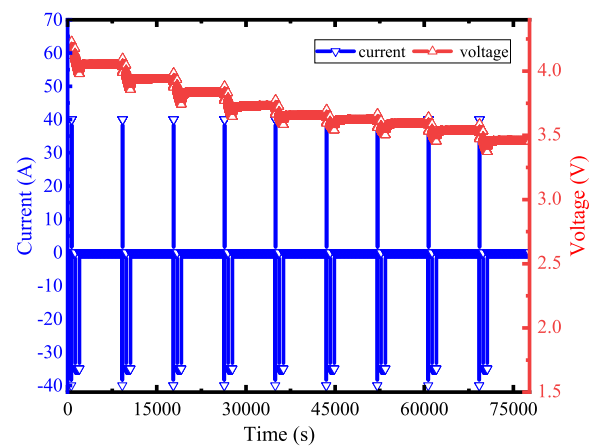
IV. EXPERIMENT AND ANALYSIS OF RESULTS

With 70Ah ternary lithium-ion battery as the research object, the working condition tests HPPC and BBDST are designed in order to verify the effectiveness of the proposed method. The test platform in the whole experiment is shown in Fig.6. Moreover, comparison and analysis are made about the identification of battery model parameters, terminal voltage prediction and SOC estimation.

Changes of current and voltage in HPPC test are shown in Fig.7. In addition, Part of the current and voltage change data of BBDST working condition test is shown in Fig.8.

A. COMPARISON OF SOC-OCV CURVE FITTING

From the part 2.1 and 2.2 mentioned above, the curve fitting quality of SOC-OCV directly affects the prior value of $U_{oc}(k)$. In order to verify the effectiveness of the segmented cubic Hermite interpolation method proposed in the paper, a comparison is made between this method and the simplified electrochemical model, SO-OCV curve fitting by polynomial
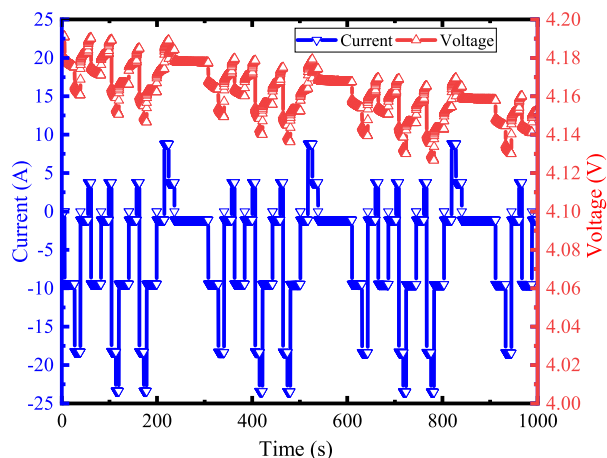
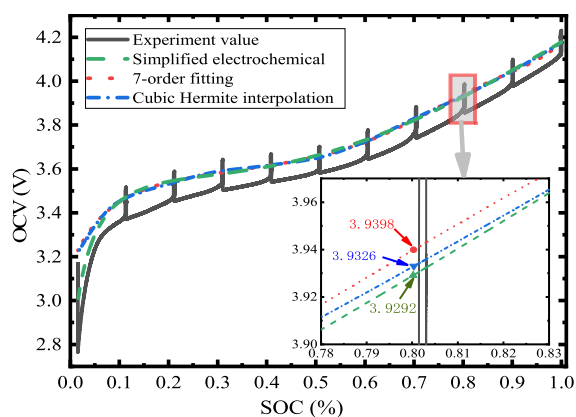**FIGURE 8.** Current and voltage values of BBDST.

FIGURE 9. SOC-OCV fitting curves.

FIGURE 10. Error of fitting.

fitting method. Fig. 9 shows the comparison results of HPPC test data fitting. The test voltage values are used to subtract the voltage values fitted by three methods, and the error curves obtained are shown in Fig.10.

From Fig. 9, all the three methods make a good description of SOC-OCV curves. However, when the data that SOC is 0.8 is enlarged, it can be find that the value of cubic Hemite Interpolation is 3.9326V, the same as the real value; the value of simplified electrochemical method is 3.9292 V with an error of 0.086%, and the value of 7-order fitting method is 3.9398 V with an error of 0.18%.

According to Fig. 10, when SOC value is less than 0.05, the fitting errors of the three methods are relatively larger because the battery is more nonlinear within the range, more sensitive to current changes. While the value of SOC approaches 0, the simplified electrochemical method is affected by the variable ln(SOC) in the equation, and there is a meaningless fit in theory. When the value of SOC is close to 1, the simplified electrochemical method is affected by the parameter ln(1-soc) in the equation, and there lies fitting situation with meaninglessness. There exists larger error in 7-order fitting method just because the accurate data of measurement points fail
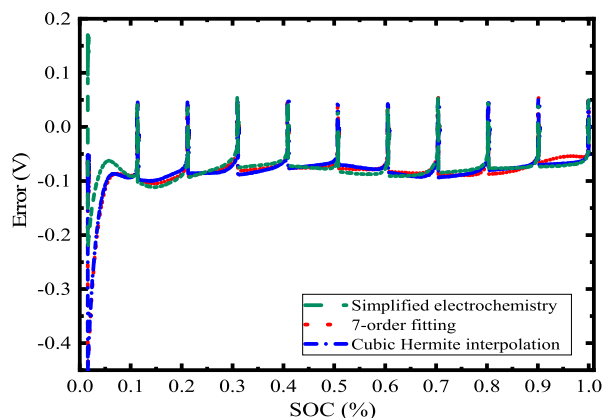
to fall on the fitting curve. The Cubic Hemite Interpolation method works well throughout the SOC change process.

B. COMPARISON OF MODEL PARAMETER IDENTIFICATION

In the sections 2.3 and 2.4, the paper derives the method of FFRLS to identify the Thevenin model and propose an improved method of adaptive forgetting factor. In order to verify the effectiveness of this method, FFRLS method and the improved method aim to identify HPPC and BBDST working conditions in section 4.1 online. The model parameters identified are used to estimate terminal voltage of the battery. The estimation results are shown in Fig. 11, where 11(a) stands for the terminal voltage estimation result under HPPC condition, and 11(b) means the terminal voltage estimation result under BBDST condition. Then with the test value subtracting, the estimated value corresponding error curve can be obtained, as shown in Fig.12, where 12(a) is the estimated error result of the terminal voltage under HPPC conditions and 12(b) the end voltage estimation error result under BBDST condition.

From Fig. 11, the method raised by the paper and FFRLS method enjoyed the good tracking effects, besides, under these two working conditions, the results estimated by different methods changed in the same way. When the forgetting factor was 1, FFRLS method was replaced by the recursive least-squares method. Nevertheless, the experiment results in the paper show that RLS method also worked well. In the experiment of HPPC, when forgetting factor was 0.9992, FFRLS method committed a larger error. While in the BBDST experiment, when forgetting factor was 0.98, the FFRLS method had a larger error too. All these situations resulted from the current mutation of charge and discharge. As shown in Fig.7, Fig.8, most of the time the current in HPPC test is in a state of continuous change or static state, requiring relatively weak model tracking capability, and forgetting factor was oriented to 1 as possible. While the current in BBDST test varied dramatically, requiring a strong model tracking capability. With the forgetting factor decreasing,
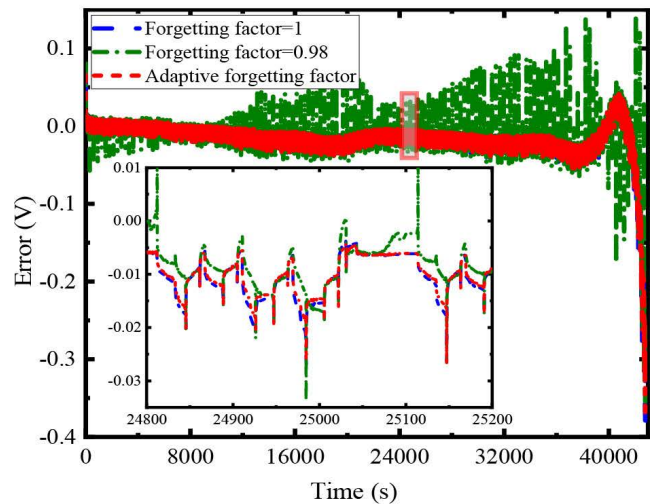
a. Terminal voltage estimation values on HPPC.

b. Terminal voltage estimation values on BBDST.
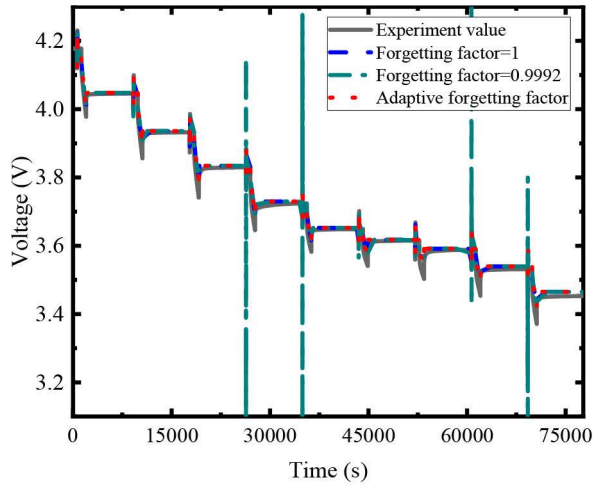
FIGURE 11. Terminal voltage estimation results.
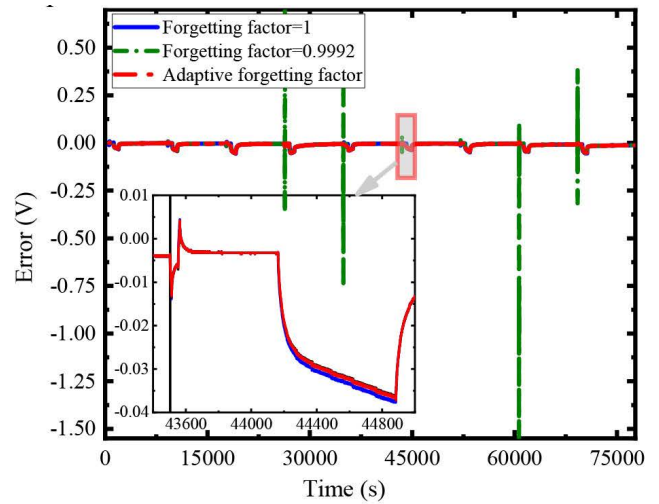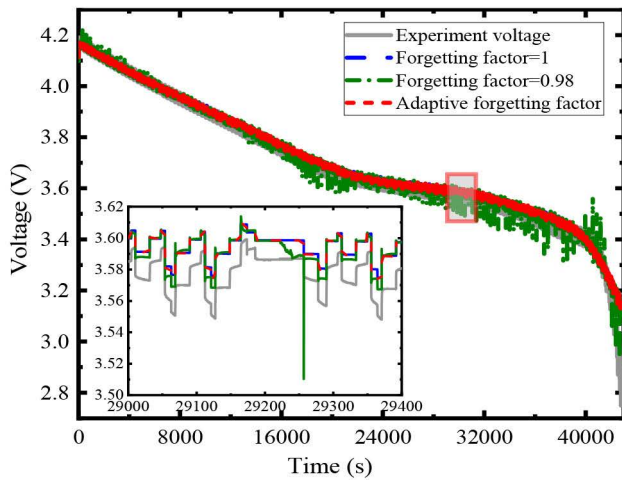
a. Terminal voltage estimation error on HPPC.

b. Terminal voltage estimation error on BBDST.

FIGURE 12. Terminal voltage estimation error results.

the fixed value of critical divergence was relatively smaller. Therefore, it is very important to select an appropriate value in FFRLS method. AFFRLS method proposed in the paper can solve such problem.

From the error results in Fig.12, estimation errors of AFFRLS method are smaller than that of FFRLS method in both working conditions. When sudden changed happen in current, the system stability was broken, though the value of forgetting factor decreased, the tracking ability of the system became stronger, and its sensitivity to noise increased, the error increased accordingly. However, with the stability of current change, the forgetting factor gradually tended to be 1, the tracking ability of the system became weaker, and the convergence estimation error became smaller. In AFFRLS method, forgetting Factor adjusted itself automatically with the change of external current input, ensuring the model accuracy at any time. But in FFRLS, forgetting factor is fixed and it failed to do the way AFFRLS method did.

According to the data in Fig.11, Fig.12, AFFRLS method proved effective in an identification of Thevenin model. Then,

to further analyze the influence of the two working conditions on the change of forgetting factor, the result of forgetting factor changing with time were plotted on two charts as shown in Fig. 13. Fig. 13(a) shows the curve of the forgetting factor under HPPC, and Fig. 13 (b) shows the curve of the forgetting factor value change under BBDST.

As shown in Fig. 13, changes in the values of forgetting factor are consistent with analysis in Fig. 11. It means that the forgetting factor changes with the current. Again, this verified the effectiveness and accuracy of AFFRLS method proposed in the paper.

C. COMPARISON OF SOC ESTIMATION

SOC estimation of lithium-ion battery proposed in the paper (see Flow Chart 5) verifies the effectiveness of RCF-UKF method. At first, Cubic Hemite Interpolation and AFFRLS method are used to identify Thevenin model, and the model
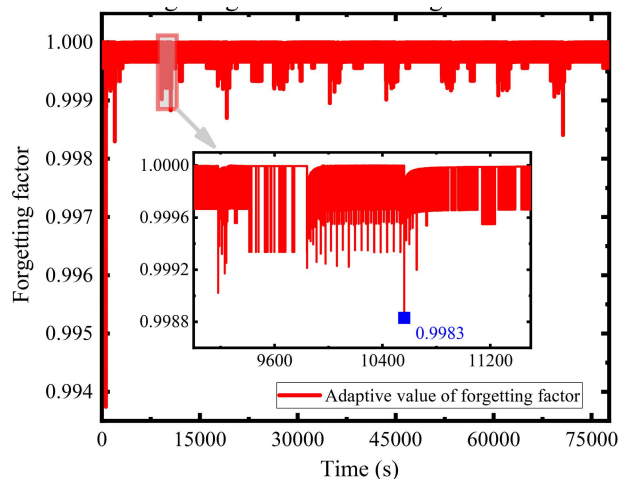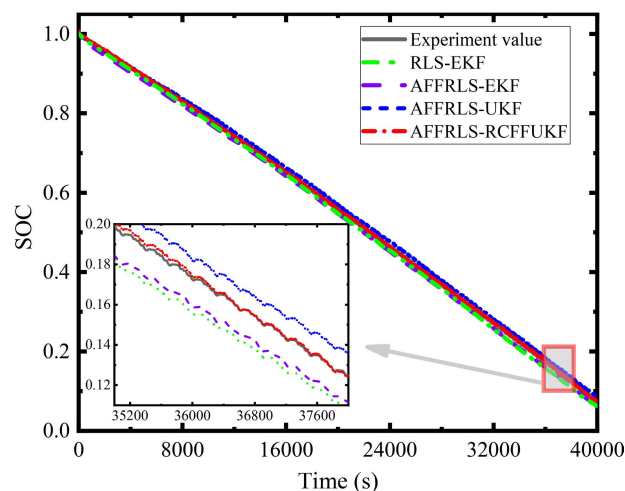
a. Change curve of forgetting factors on HPPC.
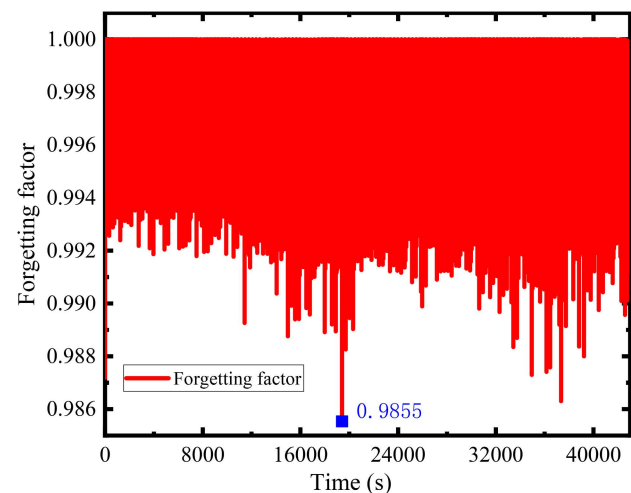
b. Change curve of forgetting factors on BBDST.

FIGURE 13. Change curves of forgetting factors.
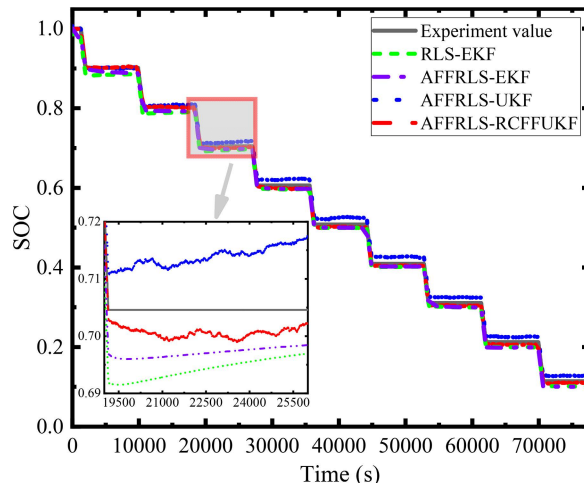
a. Estimated values of battery SOC on HPPC.

b. Estimated values of battery SOC on BBDST.

**FIGURE 14. Results of battery SOC online estimation.**

parameters are acquired to provide an accurate model for SOC estimation. Then, based on the same experimental data, methods like ampere-hour integral method, EKF method, UKF method and RCFF-UKF method were used to estimate SOC respectively. The online SOC estimation results of lithium-ion battery are shown in Fig.14, where 14(a) is the estimation value of SOC under HPPC, 14(b) is the estimation value of SOC under BBDST. Moreover, the online SOC estimation error is shown in Fig. 15, where 15(a) is the error under HPPC, 15(b) is the error under BBDST.

In Fig.14, the Experiment value curve works as the theoretical value, the value of the batery SOC calculated with the device according to the ampere-hour integral method. When the forgetting factor is 1, RLS-EKF curve represents the SOC value estimated by EKF method. Other curves represent a method of combining AFFRLS of on-line identification of model parameters suggested in the paper and SOC estimation, in which RCFFUKF is the improved UKF method proposed in the paper. From the results in Fig. 14, under the two conditions HPPC and BBDST, all the SOC results estimated

with the four methods conform to the theoretical value of SOC. While in Fig. 14(a), there exists a long time abeyance in HPPC test after discharging with a large current, and in the absence of input, state variables and observation variables change at any time, and colored noise is introduced into the state and observation. RCFFUKF method was based on the acquisition of the minimum residual array, the optimal time-varying gain array was obtained online to reduce the influence of colored noise. As a result, compared with EKF and UKF, the estimation error of this method was relatively small, and the tracking performance was much better. In Fig. 14(b), due to the interference of current changes and noise, there came the largest error in estimation error of RLS-EKF method. But the estimation error of the method raised in the paper was the smallest and tended to be stable on the whole.

Fig. 15 shows the errors of SOC estimation with four methods under HPPC and BBDST. Macroscopically, the of estimation error AFFRLS-RCFFUKF was the smallest and relatively stable. Meanwhile, the paper employed ideas in mathematical statistics like maximum error, minimum error,
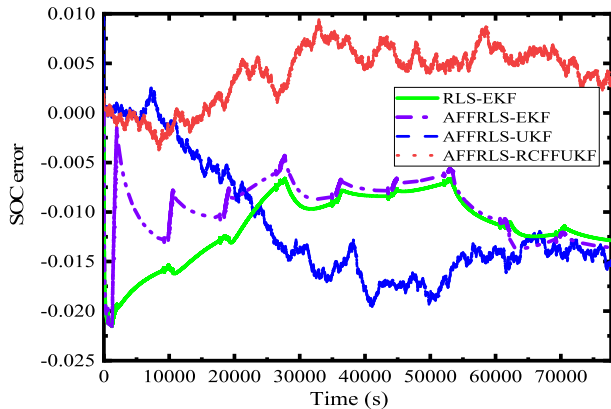
a. Estimated errors of battery SOC on HPPC.
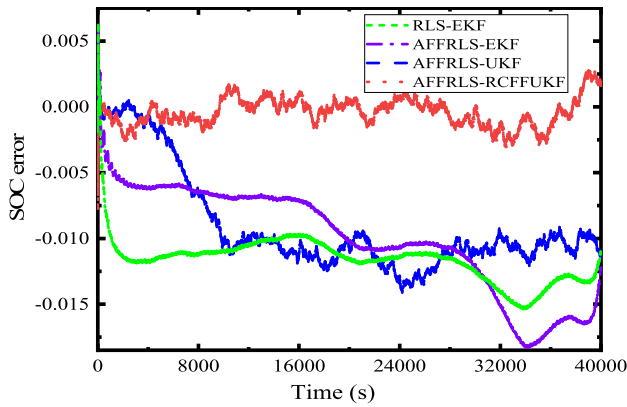
b. Estimated errors of battery SOC on BBDST.

FIGURE 15. Change curves of forgetting factors.

TABLE 1. Comparison of battery SOC estimation errors.

Condition test	Fitting method	Min error	Max error	ME	RMSE
HPPC	RLS-EKF	-0.02153	0	-0.0117	0.00369
	AFFRLS-EKF	-0.02173	0	-0.0105	0.00293
	AFFRLS-UKF	-0.01957	0.0097	0.0109	0.00407
	AFFRLS-RCFFUKF	-0.0038	0.0094	0.00391	0.00294
BBDST	RLS-EKF	-0.01538	0.0064	-0.01165	0.00176
	AFFRLS-EKF	-0.01832	0.0064	-0.01012	0.00416
	AFFRLS-UKF	-0.01416	9.1E-4	-0.00905	0.0038
	AFFRLS-RCFFUKF	-0.00811	0.0052	-4.1E-4	0.00106

mean error and RMSE indexes to have objectively analyzed the estimation results of the above methods, and the results are shown in Table 1.

Table 1 shows that under HPPC, the SOC error estimated by the algorithm of the paper lies between -0.38% and 0.948%, contrasted with other methods, the absolute maximum error was reduced by 51.5% at least, and the average error was reduced by 62.7% at least. Under BBDST,
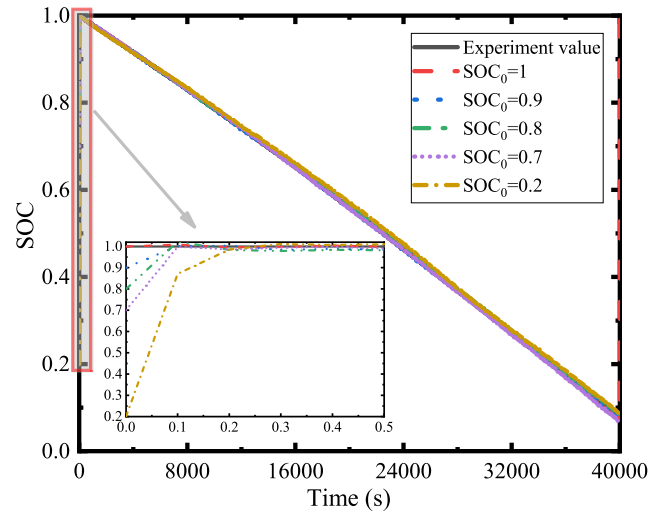

FIGURE 16. SOC estimation results at different staring SOC values.

the SOC estimation errors by the algorithm of the paper remains between -0.811% and 0.526%, and the SOC estimation errors are within 0.2% after 10 seconds of operation. Compared with other methods, the absolute maximum error is reduced by 42.7% at least, and the average error is reduced by 95% at least. The above data and analysis results proved that AFFRLS-RCFFUKF could better estimate the SOC of lithium batteries.

D. ROBUSTNESS TEST
With the initial value of SOC imprecise, a discussion is made about the convergence energy of SOC estimation method. Based on BBDST experiment, the paper analyzed the four groups of imprecise SOC initial values including 0.9, 0.8, 0.7 and 0.2, and Fig. 16 shows SOC estimation results. For a comparative analysis to be made, we draw error curves of SOC estimation before the first 10 seconds. As is shown in Fig.17

It was clear that the degree of SOC initial error affected the convergence rate. However, it was worth noting that such method can correct the SOC estimation error even when the battery was in a static state.

As is shown in Fig.17, data sampling time is 0.1s. The initial value of SOC is 0.1, the maximum estimation error is 1% after 4.5s, that is, after 45 convergent calculations. For other initial values, the estimation error has converged to 1% within 2.2s (22 calculations). Therefore, the convergence rate was pertinent to the inaccuracy of SOC initial value, but after a certain number of iterative operations, any initial error can be corrected accurately.

To discuss the adaptability of SOC estimation method to different temperatures, according to BBDST experiment, analyses are made about three groups of experiments at 15°, 25° and 35° respectively. To observe these data, some SOC estimation results are shown in Fig.18. The comparison results of SOC estimation errors are shown in Fig.19, and the statistical analysis results of the error are shown in Table 2.
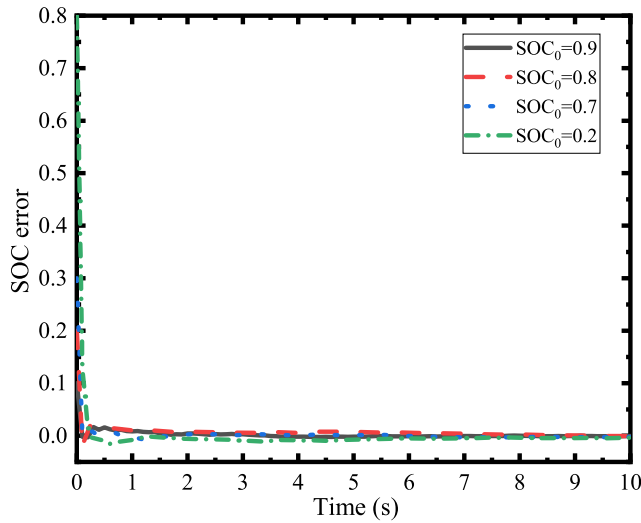
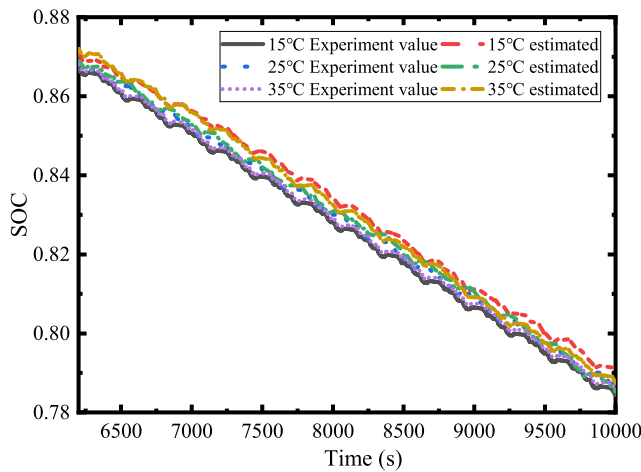FIGURE 17. SOC estimation error under different staring SOC values.

FIGURE 18. SOC estimation results at different temperatures.

TABLE 2. Comparison of battery SOC estimation errors.

Conditi on test	Fitting method	Min error	Max error	ME	RMSE
BBDST	15°C	-0.00789	0.0904	-0.00354	0.00212
	25°C	-0.00081	0.00426	-0.0004	0.00106
	35°C	-0.00619	0.00657	-0.00177	0.00224

It was obvious that the experimental value of SOC differed under the same BBDST test current condition, and that the main temperature caused a huge impact on the dynamic of the battery. The relevant SOC became small when the temperature corresponding to the open circuit voltage was a bit lower.

With the temperature at 25°, the error fluctuation stays relatively steady and the error remains relatively small, this is mainly affected by the prior value. When the temperature is at 15°, the error fluctuated greatly and the error becomes
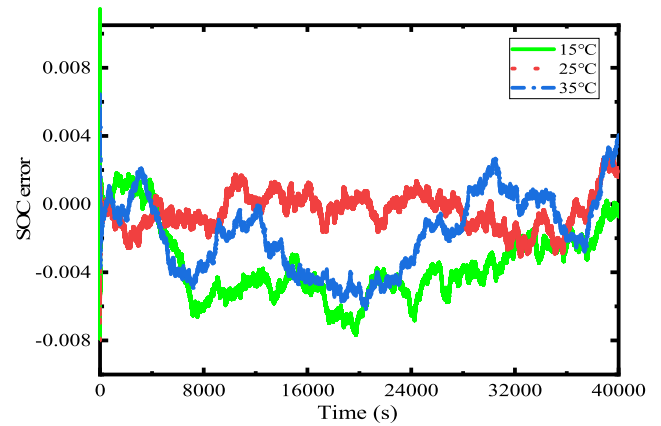

FIGURE 19. SOC estimation error at different temperatures.

relatively larger, but the average error can still keep within 0.36%. Therefore, the SOC estimation erroris affected by temperature, but after the calculation of the method proposed, the SOC estimation accuracy is relatively high, and its adaptability to different temperatures grows quite stronger.

V. CONCLUSION

The paper proposed a series of improvement measures for a higher estimation accuracy of lithium-ion battery SOC. These measures covered the polynomial fitting, the online identification of Thevenin model parameter, and the UKF SOC estimation method. These improved methods were tested under the two working conditions HPPC and BBDST, and a contrast was made between these methods with the traditional methods. The results show as follows:

1) On the basis of SOC-OCV discrete data, the segmented cubic Hermite interpolation method can be used to replace the traditional polynomial fitting method, obtaining the prior value of HPPC test terminal voltage. The segmented cubic Hermite interpolation method can keep all the interpolation points within the interpolation function, realizing the continuous smooth interpolation points, and better reflecting the real changes of HPPC test data.

2) According to Thevenin model, AFFRLS method instead of FFRLS method can be used to identify model parameters. Through comparative analysis of test data under the working conditions HPPC and BBDST, it is obvious that AFFRLS method is more accurate.

3) For the problem that the traditional UKF method is greatly affected by system noise and observation noise, the paper presented an improved UKF method with residual constraint fading memory. After comparative analysis of HPPC and BBDST test data, AFFRLS-RCFFUKF method is high in precision, good in convergence and strong in robustness in terms of SOC estimation of the battery.

The method proposed by the paper is mainly designed to solve the problem of on-line adaptive model parameter identification and SOC estimation of lithium-ion battery. And the improvements proposed are also applicable to other state estimation methods of lithium-ion battery.

REFERENCES

[1] S. Wang, S. Jin, D. Bai, Y. Fan, H. Shi, and C. Fernandez, "A critical review of improved deep learning methods for the remaining useful life prediction of lithium-ion batteries," *Energy Rep.*, vol. 7, pp. 5562–5574, Nov. 2021.

[2] X.-Y. Song, J.-Y. Huang, and J.-Q. Duan, "Estimation of state of charge of battery based on adaptive recursive least squares and unscented Kalman filtering," *Electr. Power Sci. Eng.*, vol. 35, no. 12, pp. 41–48, 2019.

[3] T. Lu and W.-Q. Yang, "Review of evaluation parameters and methods of lithium batteries throughout its life cycle," *Energy Storage Sci. Technol.*, vol. 9, no. 3, pp. 657–669, 2020.

[4] Q. Zhu, J.-X. Chen, M.-E. Xu, and C. Zou, "Iterative learning based model identification and state of charge estimation of lithium-ion battery," *IET Power Electron*, vol. 12, no. 4, pp. 852–860, 2019.

[5] G. Dong, Z. Chen, and J. Wei, "Sequential Monte Carlo filter for state-of-charge estimation of lithium-ion batteries based on auto regressive exogenous model," *IEEE Trans. Ind. Electron.*, vol. 66, no. 11, pp. 8533–8544, Nov. 2019.

[6] K. Yang, Z. Chen, and Z. He, "Online estimation of state of health for the airborne Li-ion battery using adaptive DEKF-based fuzzy inference system," *Soft Comput.*, vol. 24, no. 24, pp. 18661–18670, 2020.

[7] L. Cai, J. H. Meng, D. I. Stroe, G. Z. Luo, and R. Teodorescu, "An evolutionary framework for lithium-ion battery state of health estimation," *J. Power Sources*, vol. 412, pp. 615–622, Feb. 2019.

[8] X. Hu, H. Yuan, C. Zou, Z. Li, and L. Zhang, "Co-estimation of state of charge and state of health for lithium-ion batteries based on fractional-order calculus," *IEEE Trans. Veh. Technol.*, vol. 67, no. 11, pp. 10319–10329, Nov. 2018.

[9] C. She, L. Zhang, Z. Wang, F. Sun, P. Liu, and C. Song, "Battery state of health estimation based on incremental capacity analysis method: Synthesizing from cell-level test to real-world application," *IEEE J. Emerg. Sel. Topics Power Electron.*, early access, Sep. 14, 2021, doi: 10.1109/JESTPE.2021.3112754.

[10] Z. Wang, C. Song, L. Zhang, Y. Zhao, P. Liu, and D. G. Dorrell, "A data-driven method for battery charging capacity abnormality diagnosis in electric vehicle applications," *IEEE Trans. Transport. Electrific.*, vol. 8, no. 1, pp. 990–999, Mar. 2022, doi: 10.1109/TTE.2021.3117841.

[11] G.-L. Plett, "Review and some perspectives on different methods to estimate state of charge of lithium-ion batteries," *J. Automot. Saf. Energy*, vol. 10, no. 3, p. 249, 2019.

[12] S. Dhameja, *Electric Vehicle Battery Systems*. Amsterdam, The Netherlands: Elsevier, 2002, pp. 69–94.

[13] Z.-T. Ding, T. Deng, Z.-F. Li, and Y. Yanli, "SOC estimation of Lithium-ion battery based on ampere hour integral and unscented Kalman filer," *China Mech. Eng.*, vol. 31, no. 15, pp. 1823–1830, 2020.

[14] T. Wang, J. Yu, W.-H. Ma, F.-W. Xiao, and G.-Q. Lv, "Research progress of state of charge estimation method of battery management system," *Chin. J. Power Sources*, vol. 42, no. 2, pp. 312–315, 2018.

[15] W. Zhao, X. Kong, and C. Wang, "Combined estimation of the state of charge of a lithium battery based on a back-propagation-adaptive Kalman filter algorithm," *Proc. Inst. Mech. Eng., D, J. Automobile Eng.*, vol. 232, no. 3, pp. 357–366, 2018.

[16] J. Guo, Z. Li, and M. Pecht, "A Bayesian approach for Li-ion battery capacity fade modeling and cycles to failure prognostics," *J. Power Sources*, vol. 281, pp. 173–184, May 2015.

[17] X. Lin, Y. Tang, J. Ren, and Y. Wei, "State of charge estimation with the adaptive unscented Kalman filter based on an accurate equivalent circuit model," *J. Energy Storage*, vol. 41, Sep. 2021, Art. no. 102840.

[18] Z. Chen, H. Sun, G. Dong, J. Wei, and J. Wu, "Particle filter-based state-of-charge estimation and remaining-dischargeable-time prediction method for lithium-ion batteries," *J. Power Sources*, vol. 414, pp. 158–166, Feb. 2019.

[19] I. B. Espedal, A. Jinasena, O. S. Burheim, and J. J. Lamb, "Current trends for state-of-charge (SoC) estimation in lithium-ion battery electric vehicles," *Energies*, vol. 14, no. 11, p. 3284, Jun. 2021.

[20] C. Zhang, J. Jiang, L. Zhang, S. Liu, L. Wang, and P. Loh, "A generalized SOC-OCV model for lithium-ion batteries and the SOC estimation for LNMCO battery," *Energies*, vol. 9, no. 11, p. 900, Nov. 2016.

[21] W.-J. Fan, G.-H. Xu, B.-N. Yu, and Z.-B. Zhang, "On-line estimation method for internal temperature of lithium-ion battery based on electrochemical impedance spectroscopy," *Proc. CSEE*, vol. 41, no. 9, pp. 3283–3293, Jan. 2021.

[22] M. U. Ali, A. Zafar, S. H. Nengroo, S. Hussain, M. J. Alvi, and H.-J. Kim, "Towards a smarter battery management system for electric vehicle applications: A critical review of lithium-ion battery state of charge estimation," *Energies*, vol. 12, no. 3, p. 446, Jan. 2019.

[23] Y. Tian, R. Lai, X. Li, L. Xiang, and J. Tian, "A combined method for state-of-charge estimation for lithium-ion batteries using a long short-term memory network and an adaptive cubature Kalman filter," *Appl. Energy*, vol. 265, May 2020, Art. no. 114789.

[24] F. Yang, W. Li, C. Li, and Q. Miao, "State-of-charge estimation of lithium-ion batteries based on gated recurrent neural network," *Energy*, vol. 175, pp. 66–75, May 2019.

[25] J. Meng, G. Luo, and F. Gao, "Lithium polymer battery state-of-charge estimation based on adaptive unscented Kalman filter and support vector machine," *IEEE Trans. Power Electron.*, vol. 31, no. 3, pp. 2226–2238, Mar. 2016.

[26] Y. Xu, M. Hu, A. Zhou, Y. Li, S. Li, C. Fu, and C. Gong, "State of charge estimation for lithium-ion batteries based on adaptive dual Kalman filter," *Appl. Math. Model.*, vol. 77, no. 1, pp. 1255–1272, Jan. 2020.

[27] A. Tulsyan, Y. Tsai, R. B. Gopaluni, and R. D. Braatz, "State-of-charge estimation in lithium-ion batteries: A particle filter approach," *J. Power Sources*, vol. 331, pp. 208–223 Nov. 2016.

[28] B. Xia, C. Chen, Y. Tian, W. Sun, Z. Xu, and W. Zheng, "A novel method for state of charge estimation of lithium-ion batteries using a nonlinear observer," *J. Power Sources*, vol. 270, pp. 359–366, Dec. 2014.

[29] D. Xile, Z. Caiping, and J. Jiuchun, "Evaluation of SOC estimation method based on EKF/AEKF under noise interference," *Energy Proc.*, vol. 152, pp. 520–525, Oct. 2018.

[30] S.-L. Wang, C. Fernandez, W. Cao, C.-Y. Zou, C.-M. Yu, and X.-X. Li, "An adaptive working state iterative calculation method of the power battery by using the improved Kalman filtering algorithm and considering the relaxation effect," *J. Power Sources*, vol. 428, pp. 67–75, Jul. 2019.

[31] S. Wang, C. Fernandez, Y. Fan, J. Feng, C. Yu, K. Huang, and W. Xie, "A novel safety assurance method based on the compound equivalent modeling and iterate reduce particle-adaptive Kalman filtering for the unmanned aerial vehicle lithium ion batteries," *Energy Sci. Eng.*, vol. 8, no. 5, pp. 1484–1500, May 2020.

[32] R. Sakile and U. K. Sinha, "Estimation of lithium-ion battery state of charge for electric vehicles using an adaptive joint algorithm," *Adv. Theory Simul.*, vol. 5, Mar. 2022, Art. no. 2100397, doi: 10.1002/adts.202100397.

[33] C. Sun, H. Lin, H. Cai, M. Gao, C. Zhu, and Z. He, "Improved parameter identification and state-of-charge estimation for lithium-ion battery with fixed memory recursive least squares and sigma-point Kalman filter," *Electrochim. Acta*, vol. 387, Aug. 2021, Art. no. 138501, doi: 10.1016/j.electacta.2021.138501.

[34] J. Park, M. Lee, G. Kim, S. Park, and J. Kim, "Integrated approach based on dual extended Kalman filter and multivariate autoregressive model for predicting battery capacity using health indicator and SOC/SOH," *Energies*, vol. 13, no. 9, p. 2138, Apr. 2020.

[35] B. Jiang, H. Dai, X. Wei, and T. Xu, "Joint estimation of lithium-ion battery state of charge and capacity within an adaptive variable multi-timescale framework considering current measurement offset," *Appl. Energy*, vol. 253, Nov. 2019, Art. no. 113619.

[36] F. Liu, J. Ma, W.-X. Su, and M.-W. He, "Model parameter online identification based SOC estimation method," *J. Northeastern Univ.*, vol. 41, no. 11, pp. 1543–1549, 2020.

[37] S. Lee, J. Kim, J. Lee, and B. H. Cho, "State-of-charge and capacity estimation of lithium-ion battery using a new open-circuit voltage versus state-of-charge," *J. Power Sources*, vol. 185, no. 2, pp. 1367–1373, Dec. 2008.

[38] J. Meng, G. Luo, M. Ricco, M. Swierczynski, D.-I. Stroe, and R. Teodorescu, "Overview of lithium-ion battery modeling methods for state-of-charge estimation in electrical vehicles," *Appl. Sci.*, vol. 8, no. 5, p. 659, Apr. 2018.

[39] H.-Y. Wei, X.-J. Chen, Z.-Q. Lv, and L. Chen, "Modeling of lithium-ion battery open circuit voltage by Hermite interpolation method," *Electr. Meas. Instrum.*, vol. 55, no. 10, pp. 122–126, 2018.

[40] X. Xiong, S.-L. Wang, F. Xie, and C. Kang, "Research on parameter identification method for lithium battery based on Hermite interpolation," *Process Autom. Instrum.*, vol. 41, no. 1, pp. 10–15, 2020.

[41] J.-Q. Feng, L. Wu, K.-F. Huang, J. Lu, and X. Zhang, "Online SOC estimation of a lithium-ion battery based on FFRLS and AEKF," *Energy Storage Sci. Technol.*, vol. 10, no. 1, pp. 242–249, 2021.

[42] Z. Z. Lao, B. Z. Xia, and W. Wang, "A novel method for lithium-ion battery online parameter identification based on variable forgetting factor recursive least squares," *Energies*, vol. 11, no. 6, p. 1358, May 2018.

[43] X. Yang, S.-L. Wang, W.-H. Xu, and C.-M. Yu, "A novel lithium-ion battery SOC estimation method based on limited memory RLS and fading factor EKF algorithm," *Control Eng. China*, vol. 29, pp. 1–7, Jan. 2022.

[44] J.-S. Lim, S. Lee, and H.-S. Pang, "Low complexity adaptive forgetting factor for online sequential extreme learning machine (OS-ELM) for application to nonstationary system estimations," *Neural Comput. Appl.*, vol. 22, nos. 3–4, pp. 569–576, 2013.

[45] Y.-J. Zhang, H.-W. Wu, and C.-J. Ye, "Estimation of the SOC of a battery based on the AUKF-BP algorithm," *Energy Storage Sci. Technol.*, vol. 10, no. 1, pp. 237–241, 2021.

[46] X.-L. Zhang, Y.-T. Wang, J.-S. Xia, and Y.-Y. Zhang, "Estimation of the SOC of lithium batteries based on an improved CDKF algorithm," *Energy Storage Sci. Technol.*, vol. 10, no. 4, pp. 1454–1462, 2021.

[47] H. He, R. Xiong, and J. Peng, "Real-time estimation of battery state-of-charge with unscented Kalman filter and RTOS μCOS-II platform," *Appl. Energy*, vol. 162, pp. 1410–1418, Jan. 2016.

[48] X. Peng, Y. Li, W. Yang, and A. Garg, "Real-time state of charge estimation of the extended Kalman filter and unscented Kalman filter algorithms under different working conditions," *J. Electrochem. Energy Convers. Storage*, vol. 18, no. 4, pp. 1410–1418, Nov. 2021.

[49] D. Sun, X. Yu, C. Wang, C. Zhang, R. Huang, Q. Zhou, T. Amietszajew, and R. Bhagat, "State of charge estimation for lithium-ion battery based on an intelligent adaptive extended Kalman filter with improved noise estimator," *Energy*, vol. 214, Jan. 2021, Art. no. 119025.

[50] Z.-T. Ding, T. Deng, Z.-F. Li, and Y.-L. Yin, "SOC estimation of lithium-ion battery based on ampere hour integral and unscented Kalman filter," *China Mech. Eng.*, vol. 31, no. 15, pp. 1823–1830, 2020.

[51] W.-L. Yu, X.-L. Deng, X.-H. Yao, and J.-Z. Fu, "Thermal equilibrium test of machine tool spindle based on modified adaptive fading unscented Kalman filter," *Trans. Chin. Soc. Agricult. Machinery*, vol. 50, no. 4, pp. 363–373, 2019.

[52] H.-E. Shan, Z. Xu, and S.-H. Xi, "Improved strong tracking quadrature Kalman filtering algorithm," *Comput. Technol. Develop.*, vol. 28, no. 7, pp. 43–47, 2018.

FENG CAI received the M.S. degree in engineering and the Ph.D. degree in safety technology and engineering from the Anhui University of Science and Technology, Huainan, China, in 2005 and 2009, respectively.

Since 2009, he has been with the Anhui University of Science and Technology as a Teacher, where he is currently a Professor and a Ph.D. Supervisor. His current research interests include mine gas management technology and ventilation safety engineering. He is the Leader of the subject area of safety science and engineering, a highly effective top talent in Anhui Province, a member of the Anhui Emergency Response Expert Group, and a Visiting Scholar with West Virginia University, USA.

JING YANG received the B.S. degree in safety engineering from the Anhui University of Technology, Maanshan, China, in 2020. She is currently pursuing the M.S degree with the School of Safety Science and Engineering and the State key Laboratory of Mining Response and Disaster Prevention and Control in Deep Coal Mines, Anhui University of Science and Technology, Huainan, China. Her research interests include gas prevention and management.

SHUNLI WANG received the M.S. and Ph.D. degrees from the School of Information Engineering, Southwest University of Science and Technology, Mianyang, China. He is currently working as a Professor with the Southwest University of Science and Technology. His current research interests include modeling and state estimation strategies for lithium-ion batteries, battery pack development, and aircraft reliability. He is an Authoritative Expert in the field of new energy research and the Head of the DT Laboratory and the New Energy Measurement and Control Research Team, modeling, and state estimation methods research for lithium-ion batteries. He has undertaken more than 40 projects and 30 patents, published more than 150 research papers. He was a recipient of 20 awards, such as the Young Scholar, Science and Technology Progress Awards and the University and Enterprise Innovative Talent Team, developed multi-generational battery systems to improve the reliability and expand the application field with significant social and economic benefits.

JUQIANG FENG received the B.S. degree in automatic control from Northeastern University, Shenyang, China, in 2010, and the M.S. degree in detection technology and automatic equipment from the Southwest University of Science and Technology, Mianyang, China, in 2013. He is currently pursuing the Ph.D. degree with the State Key Laboratory of Mining Response and Disaster Prevention and Control in Deep Coal Mines, Anhui University of Science and Technology. He is a Senior Electrical Engineer. His research interests include power battery modeling and simulation on mine electric vehicles, design, and control theory of the hybrid power train.

KAIFENG HUANG received the Ph.D. degree in safety technology and engineering from the Anhui University of Science and Technology.

Since July 2017, he has been with the School of Mechanical and Electrical Engineering, Huainan Normal University, Huainan, where he is currently an Associate Professor. His research interests include machine learning, networked control systems, and fault diagnosis.

● ● ●